J|A|C|S ARTICLES

Published on Web 07/31/2009

Alkylsubstituted Thienothiophene Semiconducting Materials: Structure−Property Relationships

Mingqian He,*,§ Jianfeng Li,§ Michael L. Sorensen,§ Feixia Zhang,§ Robert R. Hancock,§ Hon Hang Fong,† Vladimir A. Pozdin,† Detlef-M. Smilgies,‡ and George G. Malliaras‡

Corning Incorporated, SP-FR-6, Corning, New York 14830, Materials Science and Engineering, Cornell University, Ithaca, New York 14853, and Cornell High Energy Synchrotron Source, Cornell University, Ithaca, New York 14853

Received May 13, 2009; E-mail: hem@corning.com

Abstract: A family of conjugated polymers with fused structures consisting of three to five thiophene rings and with the same alkyl side chains has been synthesized as a means to understand structure−property relationships. All three polymers showed well-extended conjugation through the polymer backbone. Ionization potentials (IP) ranged from 5.15 to 5.21 eV; these large values are indicative of their excellent oxidative stability. X-ray diffraction and AFM studies suggest that the polymer with the even number of fused thiophene rings forms a tight crystalline structure due to its tilted side chain arrangement. On the other hand, the polymers with the odd number of fused thiophene rings packed more loosely. Characterization in a field-effect transistor configuration showed that the mobility of the polymer with the even number of rings is 1 order of magnitude higher than its odd-numbered counterparts. Through this structure−property study, we demonstrate that proper design of the molecules and properly arranged side chain positions on the polymer backbone can greatly enhance polymer electronic properties.

1. Introduction

Organic semiconducting materials are attractive for use in many components of electronic devices, due to many fundamental advantages over their inorganic counterparts in achieving low-cost, large-area, and mechanically flexible electronics.[1,2] Many organic conjugated small molecules, such as acenes and heteroacenes, have been explored to achieve high organic field effect transistor (OFET) mobility over the past decade.[3,4] Although hole mobility upward of 43 cm/(V•s) has been achieved by single crystal small molecule devices,[5,6] obvious drawbacks such as poor solubility, nontrivial processing methods, and environmental and oxidative stability issues have hindered the use of small molecules in real applications. During the past several years, some novel organic small molecules were designed and synthesized for OFET applications in our laboratory.[7] Our intentions are (1) to design and synthesize more environmentally stable OFET molecules, (2) to design and synthesize molecules which could be polymerized for using easy solution processing methods, and (3) to achieve mobility close to that of amorphous silicon.

A series of β-alkylsubstituted fused thiophene compounds was successfully synthesized and reported by us 2 years ago.[7] We have found that these thienothiophene compounds, whose number of fused thiophene rings varies from three to seven members, can form very regular layered structures in their single crystal formats, which exhibit great potential for OFET applications. Compared with fused benzenes such as pentacene, the UV−vis absorptions of fused thiophenes demonstrate large blue-shifts which indicate they are more stable with regard to oxidation.[8,9] Since we intentionally added alkyl groups to the β positions, these fused thiophenes also show great improvement in solubility and processability. In addition, all of these fused thiophenes have their α-positions available, so that they can be easily converted into different polymers.

During the past several years, thienothiophene polymer materials such as poly(2,5-bis(3-alkylthiophene-2-yl)thieno[3,2-b]thiophene)s (PBTTTs),[10−15] poly(2,5-bis(3-alkyl-5-(3-alkylthio-

§ Corning Incorporated.
† Materials Science and Engineering, Cornell University.
‡ Cornell High Energy Synchrotron Source, Cornell University.

(1) Allard, S.; Forster, M.; Souharce, B.; Thiem, H.; Scherf, U. *Angew. Chem., Int. Ed.* **2008**, *47*, 4070.
(2) Sirringhaus, H.; Brown, P. J.; Friend, R. H.; Nielsen, M. M.; Bechgaard, K.; Langeveld-Voss, B. M. W.; Spiering, A. J. H.; Janssen, R. A. J.; Meijer, E. W.; Herwig, P.; de Leeuw, D. M. *Nature* **1999**, *401*, 685.
(3) Anthony, J. *Chem. Rev.* **2006**, *106*, 5028.
(4) Liu, S.; Wang, W. M.; Briseno, A. L.; Mannsfeld, S. C. B.; Bao, Z. *Adv. Mater.* **2009**, *21*, 1217.
(5) (a) Podzorov, V.; Menard, E.; Borissov, A.; Kiryukhin, V.; Rogers, J. A.; Gershenson, M. E. *Phys. Rev. Lett.* **2004**, *93*, 086602. (b) Sundar, V. C.; Zaumseil, J.; Podzorov, V.; Menard, E.; Willett, R. L.; Someya, T.; Gershenson, M. E.; Rogers, J. A. *Science* **2004**, *303*, 1644.
(6) Yamagishi, M.; Takeya, J.; Tominari, Y.; Nakazawa, Y.; Kuroda, T.; Ikehata, S.; Uno, M.; Nishikawa, T.; Kawase, T. *Appl. Phys. Lett.* **2007**, *90*, 182117.
(7) He, M.; Zhang, F. *J. Org. Chem.* **2007**, *72*, 442.
(8) Zhang, X.; Cote, A. P.; Matzger, A. *J. Am. Chem. Soc.* **2005**, *127*, 10502.
(9) Mazaki, Y.; Kobayashi, K. *Tetrahedron Lett.* **1989**, *25*, 3315.
(10) McCulloch, I.; Heeney, M.; Bailey, C.; Genevicius, K.; Macdonald, I.; Shkunov, M.; Sparrowe, D.; Tierney, S.; Wagner, R.; Zhang, W.; Chabinyc, M. L.; Kline, R. J.; McGehee, M. D.; Toney, M. F. *Nat. Mater.* **2006**, *5*, 328.
(11) McCulloch, I.; et al. *Adv. Mater.* **2009**, *21*, 1091.

 10.1021/ja903895s CCC: $40.75

phen-2-yl)thiophen-2-yl)thiazolo[5,4-*d*]thiazole)s (PTzQTs),[16,17] poly(didodecylquaterthiophene-alt-didodecylbithiazole (PQT-BTz-C12)[18] and poly(2,5-bis(thiophene-2-yl)-(3,7-ditridecanyltetrathienoacene) (P2TDC13FT4)[19] have been reported with high charge carrier mobility, improved oxidative stability and improved processability. More recently, naphthalenedicarboximide and indenofluorenedicyanovinylene-based ladder-type polymers were reported as high performance n-type semiconducting materials.[20,21] These "second generation" materials allow organic polymeric materials now to compete with amorphous silicon (a:Si) in the market of low-end electronics such as RFIDs, backplanes for electrophoretic displays (EPD) and organic photovoltaic (OPV) applications.[22]

PBTTT and P2TDC13FT4 polymers both have demonstrated that thienothiophene related polymer semiconductor materials have great potential for real commercial applications. It is of major interest to understand why fused thiophene polymers perform so well as organic semiconducting materials. For PBTTT polymers, the high mobilities were due to these polymers forming liquid crystalline phases in the postannealing process, which improved the formation of the lamellar structure, and greatly enhanced polymer packing behavior.[10−15] No liquid crystalline phases had been observed in the P2TDC13FT4 polymer postannealing process; however, lamellae packing was clearly identified.[19]

High mobility polymer thin films of P2TDC13FT4 can be easily obtained without a careful postannealing process. This difference may be due to tetrathienoacene (FT4) having a much larger conjugated unit size than a two-member fused thiophene. Larger units can easily form $\pi-\pi$ stacking without the assistance from forming liquid crystalline phases. However, McCulloch et al. recently reported that thienothiophene (FT2) polymers can also achieve mobility similar to FT4 polymers.[11] This work raises a host of very interesting questions: Does the size of the conjugated unit matter? What is the best unit size for fused thiophenes to obtain the best device performance? Do odd-numbered and even-numbered fused rings have any impact on device behavior? Since the odd-numbered fused thiophenes have their side chains on the same side of the fused thiophene ring, what is the side chain effect?

Recently, Kline et al.[23] indicated that an optimal side chain density and uniformity can promote side chain packing and interdigitation which can greatly improve conjugated polymer backbone arrangements. A highly ordered polymer backbone from strong π stacking and higher lamellar ordering resulted in better OFET performance. What is the relative importance of side chain direction and fused ring size?

To answer all of these important questions, we believe that a structure−property relationship study of systematically designed fused thiophene ring compounds with varied conjugation sizes is warranted. Such a study can certainly guide us to properly design OFET molecules. Three polymers, poly(2,5-bis(thiophene-2-yl)-(3,5-didecanyltrithienoacene) (P2TDC10FT3), poly(2,5-bis(thiophene-2-yl)-(3,7-didecanyltetrathienoacene) (P2TDC10FT4), and poly(2,5-bis(thiophene-2-yl)- (3,6-didecanylpentathienoacene) (P2TDC10FT5), have been successfully synthesized in our laboratory. Polymers having the same side chain lengths were chosen for more accurate and meaningful comparison. Although we have noticed that the side chain length has significant impact on the charge carrier mobility, we did not select the best performing polymers for comparison due to synthetic convenience. Side chain length effects will be reported in the future.

2. Experimental Section

Synthesis of Materials. Monomers **1**, **2**, and **3** were synthesized according to our previous papers.[7,19] Three polymers, namely, poly(2,5-bis(thiophene-2-yl)-(3,5-didecanyltrithienoacene) (P2TDC10FT3), poly(2,5-bis(thiophene-2-yl)-(3,7-didecanyltetrathienoacene) (P2TDC10FT4), and poly(2,5-bis(thiophene-2-yl)-(3,6-didecanylpentathienoacene) (P2TDC10FT5), were synthesized using the following procedures (Scheme 1).

Poly(2,5-bis(thiophene-2-yl)-(3,5-didecanyltrithienoacene) (P2TDC10FT3). 2,6-Dibromo-3,5-didecanyltrithienoacene (1.0 g, 1.57 mmol) **1** and 1,1′-[2,2′-bithiophene]-5,5′-diylbis[1,1,1-trimethylstannane] (0.77 g, 1.57 mmol) **4** were dissolved into toluene (30 mL) in a flask. Nitrogen was bubbled through this flask for a few minutes. Tetrakis(triphenylphosphine)palladium(0) (0.09 g, 0.785 mmol) was added to this mixture. This flask was heated to 125 −130 °C under nitrogen overnight before being poured into a methanol (400 mL) and concentrated hydrochloric acid (20 mL) solution and stirred overnight at room temperature. The precipitate was filtered and extracted in a Soxhlet with acetone and hexane for 24 h each. The obtained polymer was then dissolved into chlorobenzene and filtered and precipitated in methanol. The collected polymer was dried in vacuum to yield 0.92 g (87.6%). ^{1}H NMR in tetrachloroethane can be found in Supporting Information. Element analysis: theoretical, C, 67.45; H, 7.55; S 25.01; experimental, C, 66.84; H, 6.96; S, 24.39.

Poly(2,5-bis(thiophene-2-yl)-(3,7-didecanyltetrathienoacene) (P2TDC10FT4). Following the above procedure, compounds **2** (1.0 g, 1.45 mmol), **4** (0.71 g, 1.45 mmol), and $Pd(PPh_3)_4$ (0.084 g,

(12) Hamadani, B. H.; Gundlach, D. J.; McCulloch, I.; Heeney, M. *Appl. Phys. Lett.* **2007**, *91*, 243512.
(13) Chabinyc, M. L.; Toney, M. F.; Kline, R. S.; McCulloch, I.; Heeney, M. *J. Am. Chem. Soc.* **2007**, *129*, 3226.
(14) Umeda, T.; Tokito, S.; Kumaki, D. *J. Appl. Phys.* **2007**, *101*, 054517.
(15) (a) Kline, R. J.; DeLongchamp, D. M.; Fischer, D. A.; Lin, E. K.; Heeney, M.; McCulloch, I.; Toney, M. F. *Appl. Phys. Lett.* **2007**, *90*, 062117. (b) Lucas, L. A.; DeLongchamp, D. M.; Vogel, B. M.; Lin, E. K.; McCulloch, I.; Heeney, M.; Jabbour, G. E. *Appl. Phys. Lett.* **2007**, *90*, 012112.
(16) Osaka, I.; Zhang, R.; Sauvé, G.; Smilgies, D.-M.; Kowalewski, T.; McCullough, R. D. *J. Am. Chem. Soc.* **2009**, *131*, 2521.
(17) Osaka, I.; Sauvé, G.; Zhang, R.; Kowalewski, T.; McCullough, R. D. *Adv. Mater.* **2007**, *19*, 4160.
(18) Kim, D. H.; Lee, B.-L.; Moon, H.; Kang, H. M.; Jeong, E. J.; Park, J.-I.; Han, K.-M.; Lee, S.; Yoo, B. W.; Koo, B. W.; Kim, J. Y.; Lee, W. H.; Cho, K.; Becerril, H. A.; Bao, Z. *J. Am. Chem. Soc.* **2009**, *131*, 6124.
(19) Fong, H. H.; Pozdin, V. A.; Amassian, A.; Malliaras, G. G.; Smilgies, D.-M.; He, M.; Gasper, S.; Zhang, F.; Sorensen, M. *J. Am. Chem. Soc.* **2008**, *130*, 13202.
(20) (a) Yan, He.; Chen, Z.; Zheng, Y.; Newman, C.; Quinn, J. R.; Dötz, F.; Kastler, M.; Facchetti, A. *Nature* **2009**, *457*, 679. (b) Chen, Z.; Zheng, Y.; Yan, H.; Facchetti, A. *J. Am. Chem. Soc.* **2009**, *131*, 8.
(21) (a) Hakan, U.; Chad, R.; Wang, Z.; Huang, H.; Deliomeroglu, Murat., K.; Zhukhovitskiy, A.; Facchetti, A.; Marks, T. J. *J. Am. Chem. Soc.* **2009**, *131*, 5586. (b) Hakan, U.; Facchetti, A.; Marks, T. J. *J. Am. Chem. Soc.* **2008**, *130*, 8580.
(22) (a) Loo, Y.-L.; McCulloch, I. *MRS Bull.* **2008**, *33*, 653. (b) *Organic Field-Effect Transistors*, 1st ed.; Bao, Z., Locklin, J., Eds.; CRC Press: Boca Raton, FL, 2007. (c) *Organic Electronics: Materials, Manufacturing and Applications*; Klauk, H., Ed.; Wiley-VCH: Weinheim, Germany, 2006. (d) *Semiconducting Polymers: Chemistry, Physics and Engineering*; Hadziioannou, G., Malliaras, G. G., Eds.; Wiley-VCH: Weinheim, Germany, 2007. (e) Sirringhaus, H.; Tessler, N.; Friend, R. H. *Science* **1998**, *280*, 1741–1744. (f) Huitena, H. E. A.; Gelinck, G. H.; van der Putter, J. B. P. H.; Kuijk, K. E.; Hart, C. M.; Cantatore, E.; Herwig, P. T.; van Breemen, A. J. J. M.; de Leeuw, D. M. *Nature* **2001**, *414*, 599. (g) Bao, Z. *Adv. Mater.* **2000**, *12*, 227–230. (h) Li, Y. N.; Wu, Y. L.; Ong, B. S. *Macromolecules* **2006**, *39*, 6521.
(23) Kline, R. J.; DeLongchamp, D. M.; Fischer, D. A.; Lin, E. K.; Richter, L. J.; Chabinyc, M. L.; Toney, M. F.; Heeney, M.; McCulloch, I. *Macromolecules* **2007**, *40*, 7960.

Scheme 1. Synthesis of Thienothiophene Polymers

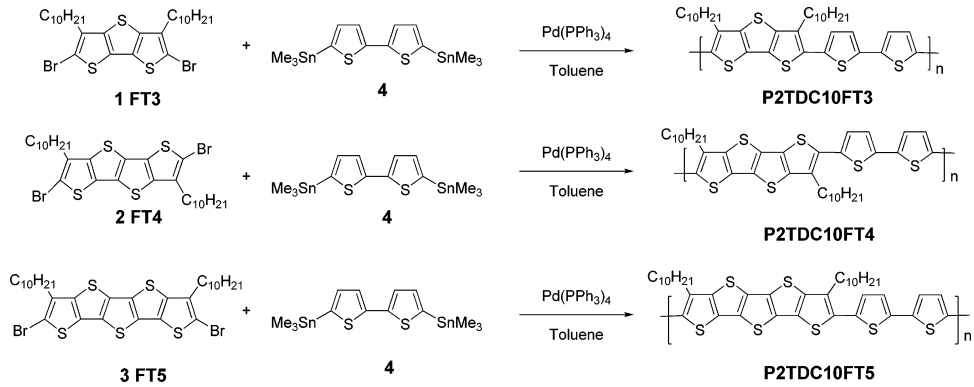

0.073 mmol) were reacted in toluene (30 mL) under nitrogen. Polymer obtained from purification was 0.97 g (92.4%). ^{1}H NMR in tetrachloroethane can be found in Supporting Information. Element analysis: theoretical, C, 65.46; H, 6.94; S, 27.60; experimental, C, 64.84; H, 6.46; S, 26.94.

Poly(2,5-bis(thiophene-2-yl)-(3,6-didecanylpentathienoacene) (P2TDC10FT5). Following the above synthetic procedure, compounds **3** (0.75 g, 1.00 mmol), **4** (0.49 g, 1.00 mmol), and $Pd(PPh_3)_4$ (0.058 g, 0.05 mmol) were reacted in toluene (30 mL) under nitrogen. Polymer obtained from purification was 0.69 g (88.5%). ^{1}H NMR in tetrachloroethane can be found in Supporting Information. Element analysis: theoretical, C, 63.78; H, 6.42; S, 29.80; experimental, C, 63.18; H, 6.01; S, 29.80.

Trace metal analysis indicated all polymers contain tin and palladium residues.

Characterization Measurements. Polymers were characterized by elemental analysis using a CE Elantech FlashEA 1112 Series CNHS-O analyzer. Polymer molecular weights were evaluated via gel permeation chromatography (GPC) using a Waters Alliance 2690 separation module with a Styragel HT3 column (4.6 × 300 mm, 10 μm, 500−30 000 molecular weight range) and a Styragel HT6E column (4.6 × 300 mm, 10 μm, 5000−10 000 000 molecular weight range) connected in series. Detection was completed by a Waters Model 2410 Refractive Index Detector and a Waters Model 996 Photodiode Array Detector. Calibrations were carried out with external polystyrene standards, Easi-Cal PS-2 A and B (Polymer Laboratories, Ltd.) at 0.1% (w/v) in toluene. The mobile phase was 1,2-dichlorobenzene with a flow rate of 0.5 mL/min and a column temperature of 35 °C. Samples were prepared at a concentration of 1 mg/mL in dichlorobenzene. Injection volume was 50 μL.

Cyclic voltammetric measurements were performed on a Pine Instrument Wavenow system with a three-electrode cell. The working electrode was coated with a polymer thin film from a polymer solution in pentachloroethane in an electrolyte solution of tetrabutylammonium hexafluorophosphate ($TBAHPF_6$) in HPLC grade acetonitrile (0.1 M). Ag/AgCl electrode, platinum wire, and polymer-coated glassy carbon were used as reference, counter, and working electrodes, respectively. A 10 μL sample of 0.5% by weight solution of each polymer was drop cast onto the glassy carbon to form a thin film. The electrode was then dried in a vacuum oven before insertion into the cell. The ionization potential value (IP) (E_{HOMO}) was estimated using the equation $E_{HOMO} = E_{OX} + 4.4$, where E_{OX} is the onset potential of oxidation versus SCE.[24]

Grazing Incidence Wide Angle X-ray Scattering (GIWAXS) was performed on the samples at the D1 station of the Cornell High Energy Synchrotron Source (CHESS). A wide bandpass (1.5%) double-bounce multilayer monochromator defined a 10.0 keV photon beam. Samples were studied under various incident angles ranging from above the critical angle of the thin film to slightly above the critical angle of the silicon oxide substrate. This was done in order to optimize the scattering from the thin film with minimal substrate reflections. Scattering intensities were recorded using a 2-D area detector (MedOptics). Working sample to detector distances were 89, 88, and 91 mm for P2TDC10FT3, P2TDC10FT4, and P2TDC10FT5, respectively. Scattering vectors were calculated[25] and refraction corrected.[26]

Tapping-mode atomic force microscopy (AFM) was carried out on a Veeco Dimension 3100 atomic force microscope. The AFM observations were performed at room temperature in air using RTESPW etched silicon probe with nominal spring constant of 40 N/m and nominal resonance frequency of 250 Hz. A typical value of AFM detector signal, corresponding to an rms cantilever oscillation amplitude, was equal to ~1 V, and the images were acquired at 1 Hz scan frequency in 5 × 5 μm^2 and 1 × 1 μm^2 scan areas.

Fabrication and Characterization of OFET Devices. Top-contact bottom-gate transistors using P2TDC10FTn (n = 3, 4, 5) as the organic semiconducting channel were fabricated in ambient conditions. Heavily doped Si⟨100⟩ wafers were used as gate electrodes with a 300 nm thermally grown silicon dioxide layer as the gate dielectric. The substrates were cleaned by sonication in semiconductor grade acetone and isopropyl alcohol for 10 min in each solvent, and then given a 15 min air plasma treatment. Hexamethyldisilazane (HMDS, ≥99%) and vaporized octyltrichlorosilane (C8OTS) were used for surface modification of the gate dielectric layer. Prior to the SAM treatment, precleaned Si/SiO_2 samples were baked at 200 °C for 15 min in N_2 for dehydration.

Solutions of polymers in pentachloroethane (3 mg/mL) were prepared by heating to 170 °C for 30 min with stirring to speed up dissolution. Polymer films were then deposited by spin-coating at 1500 rpm for 40 s. The films were baked at 150 °C in a vacuum chamber to remove the solvent prior to thermal evaporation of top contacts. Gold contacts (50 nm) for source and drain electrodes were vacuum-deposited at a rate of 2.5 Å/s through a metal shadow mask that defined a series of transistor devices with a channel length (L) of 80 μm and a channel width (W) of 1 mm. Polymeric transistors were characterized in air using the Cascade Microtech Model 12861B probe station and Keithley 4200-SCS Semiconductor Characterization System.

When measuring current−voltage curves and transfer curves, the gate voltage (V_G) was scanned from +20 to −80 V. The mobility was evaluated from the saturation regime with a source-drain voltage (V_{SD}) = −80 V using the following equation:

(24) Agrawal, A. K.; Jenekhe, S. A. *Chem. Mater.* **1996**, *8*, 579.

(25) WAXS / GIWAXS @ D1: Conversions: http://staff.chess.cornell.edu/~smilgies/D-lineNotes/GISAXS-at-D-line/GIWAXS@D1_Conversions.html.

(26) (a) Busch; et al. *J. Appl. Crystallogr.* **2006**, *39*, 433. (b) Breiby; et al. *J. Appl. Crystallogr.* **2008**, *41*, 262.

$$I_{DS,sat} = \frac{W}{2L}\mu_i C_r (V_G - V_{TH})^2 \quad (1)$$

where I_{DS} is the drain current, C_r is the capacitance per unit area of the gate dielectric layer, V_G is the gate voltage, and V_{TH} is the threshold voltage. V_{TH} was determined from the intercept in the plot of $(I_{DS})^{1/2}$ vs V_G.

3. Results and Discussions

Material Properties. Gel Permeation Chromatography (GPC). Polymer molecular weights were evaluated by GPC. The results are listed in Table 1.

GPC results indicated that only the P2TDC10FT4 polymer has a narrowly distributed molecular weight. Its polydisperity is only 1.23. However, both the P2TDC10FT3 and P2TDC10FT5 polymers generated broader peaks in the GPC system. We have noticed that the P2TDC10FT4 monomer is less soluble when compared with the P2TDC10FT3 and P2TDC10FT5 monomers. Since P2TDC10FT3 and P2TDC10FT5 have much stronger dipole moments, they tend to pack in an up and down fashion. This type of packing can compensate for their molecular charge distribution. The single crystal structure proved this assumption. On the other hand, P2TDC10FT4 has a different molecular symmetry which resulted in easier to form $\pi-\pi$ molecular aggregation.

Therefore, both P2TDC10FT3 and P2TDC10FT5 demonstrated much better solubility than their counterpart P2TDC10FT4 molecules. As a result, when the polymers were synthesized, both the P2TDC10FT3 and P2TDC10FT5 polymers had much higher molecular weights. However, both polymers also gave much broader molecular weight distributions and sometimes their distributions appeared bimodal. Initially, these results led us to question the purity of the P2TDC10FT3 and P2TDC10FT5 monomers or that there was a problem with our synthesis. After many trials, we are now sure that our monomers are pure and the synthesis is the same as that used for the P2TDC10FT4 polymer synthesis. We suspect that the bimodal molecular weight distributions come from a mismatch of P2TDC10FT3 and P2TDC10FT5 polymer structures with the GPC polystyrene standard.

UV−Vis and Cyclic Voltammetry. Polymers were dissolved into chloroform for solution absorption studies. Thin film absorption studies were conducted by spin coating chlorobenzene polymer solutions on quartz glass. Results are shown in Figure 1.

The absorption maxima for P2TDC10FT3, P2TDC10FT4, and P2TDC10FT5 polymers in solution are 511, 498, and 522 nm, respectively. Aside from a narrow absorption maximum at 498 nm, P2TDC10FT4 also showed a second peak at 584 nm. Compared with DC10FT4 and DC10FT5 small molecules, all polymer solutions showed large red-shifts which demonstrated that all polymers have extended their conjugation through polymer chain formation. For thin film absorption spectra, the absorption maxima for the P2TDC10FT4 polymer were largely red-shifted relative to solution phase values. The maximum absorption appears at 545 nm with the 584 nm shoulder absorption being unshifted. This large absorption maximum red-shift suggested that the P2TDC10FT4 polymer can easily form $\pi-\pi$ stacking structures through its conjugated polymer backbone in the solid state. On the other hand, a small red-shift is observed for the P2TDC10FT3 polymer and no shift is observed for the P2TDC10FT5 polymer. These results demonstrated that odd fused ring polymer systems do not show enhanced $\pi-\pi$ stacking in the solid state.

Table 1. Molecular Weight of P2TDC10FT3, P2TDC10FT4, and P2TDC10FT5

polymer	M_n	M_w	polydispersity
P2TDC10FT3	26285	51227	1.94
P2TDC10FT4	13142	16194	1.23
P2TDC10FT5	22922	52373	2.28

Initially, we speculated that this is due to the following reason: similar to the DC10FT4 single crystal structure,[7] P2TDC10FT4 polymer side chains crystallize in the solid state and form side chain interdigitated structures which enhance the polymer backbone $\pi-\pi$ stacking. However, DSC results did not confirm this assumption, since no phase transitions were observed. Comparing DC10FT4 structure with both DC10FT3 and DC10FT5 compounds, DC10FT4 has its side chains pointing to opposite directions. When P2TDC10FT4 polymer backbone comes to pack, there is less chance to be interfered by side chains which resulted in tighter lamellae distance (see below) and better $\pi-\pi$ packing. On the other hand, both P2TDC10FT3 and P2TDC10FT5 have their side chains at the same side. To compensate for their molecular charge distribution, the polymer backbones need to adopt an up and down packing motif. This motif causes side chain interference which resulted in large lamellar spacing. Our X-ray results (see below) corroborated this interpretation. In addition, the energy band gap (E_g) was calculated from the thin film onset absorption spectra, and data are listed in Table 2.

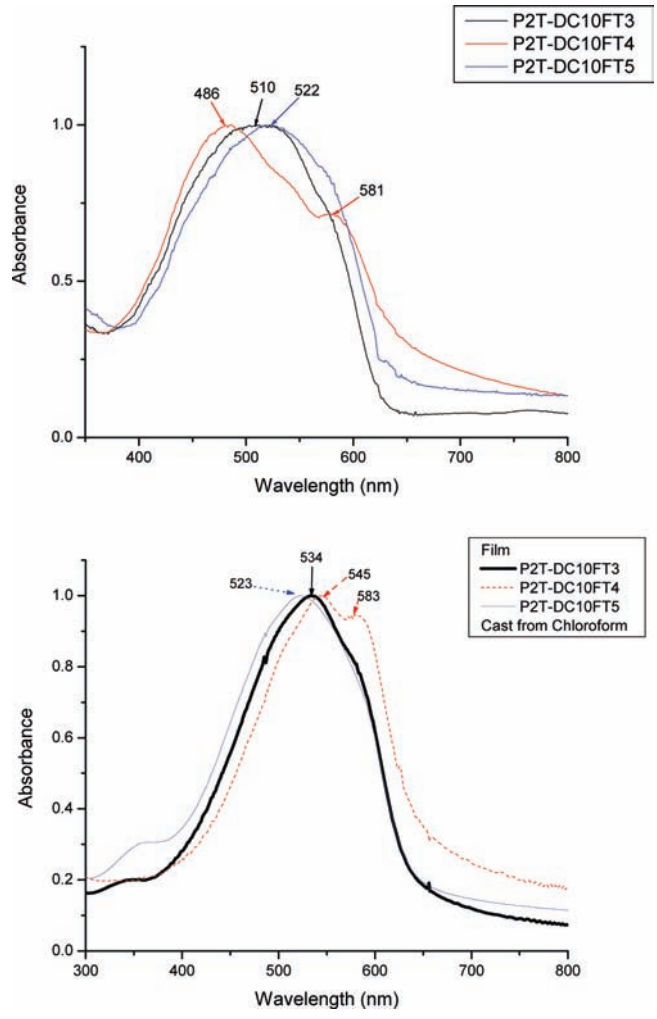

Figure 1. UV−vis spectra of FT polymers: solution and thin film.

Table 2. Absorption Maxima, Energy Band Gap, and Ionization Potential Energy Values of FT Polymers

polymer	λ_{max} (nm)	E_g (eV)	IP (eV)
P2TDC10FT3	534	1.9	5.15
P2TDC10FT4	545	1.8	5.20
P2TDC10FT5	523	1.9	5.21

Cyclic voltammetry (CV) was also used to study the polymer thin films oxidation potential. Data are also listed in Table 2.

Both polymer P2TDC10FT3 and P2TDC10FT5 have the same energy band gap of 1.9 eV. The P2TDC10FT4 polymer has an energy band gap at 1.8 eV. These band gaps are smaller than that of rrP3HT (2.0 eV) and slightly higher than or the same as that of PTzQT (1.8 eV).[16] The values of ionization potential (IP) (E_{HOMO}) for thin films were calculated from the onset of the oxidation potentials from the cyclic voltammetry of the polymer films as shown in Figure 2. P2TDC10FT3, P2TDC10FT4, and P2TDC10FT5 polymer films gave the IP values of 5.15, 5.20, and 5.21 eV, respectively. All of these values are larger than those of rrP3HT (4.9 eV), PBTTT (5.1 eV), and PTzQT (5.1 eV).[16] The larger IP values indicate that P2TDC10FT*n* (n = 3, 4, 5) polymers are more stable against oxidation. It seems that thiophenes with a higher number of fused ring are more stable.

Thermal Analysis. Polymer thermal stability was investigated by thermal gravimetric analysis (TGA). All three polymers were heated to 600 °C at a rate of 10 °C/min in a nitrogen atmosphere to observe their decomposition temperatures. Although there are slight differences of the temperatures of the onset of decomposition for the three polymers, all three polymers showed great stability up to 400 °C, which provides a broad operation window for semiconducting processes.

Polymer thermal behavior was also evaluated by differential scanning calorimetry (DSC). DSC analysis was performed at a rate of 5 °C/min to observe any possible phase transitions. Second heating and cooling cycles were recorded in order to eliminate artifacts due to water or solvent outgassing. Unlike DSC results for PBTTT polymers,[10,11] there are few features in these polymer DSC diagrams. No obvious endothermic and exothermic peaks were observed from the P2TDC10FT3, P2TDC10FT4, and P2TDC10FT5 polymers (Figure 3).

The polymers were also studied under polarized light microscopy in transmission using a Nikon Optiphot-Pol microscope. Samples of the polymers were placed on microscope glass substrates and heated to 180 −200 °C. At this point, the polymer changed from a powder to a soft solid. Once softened, a cover glass was placed on top and pressed down, followed by quickly

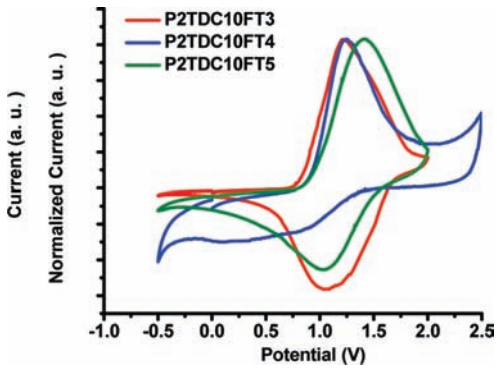

Figure 2. Cyclic voltammetry measurements of FT3, FT4, and FT5 polymers.

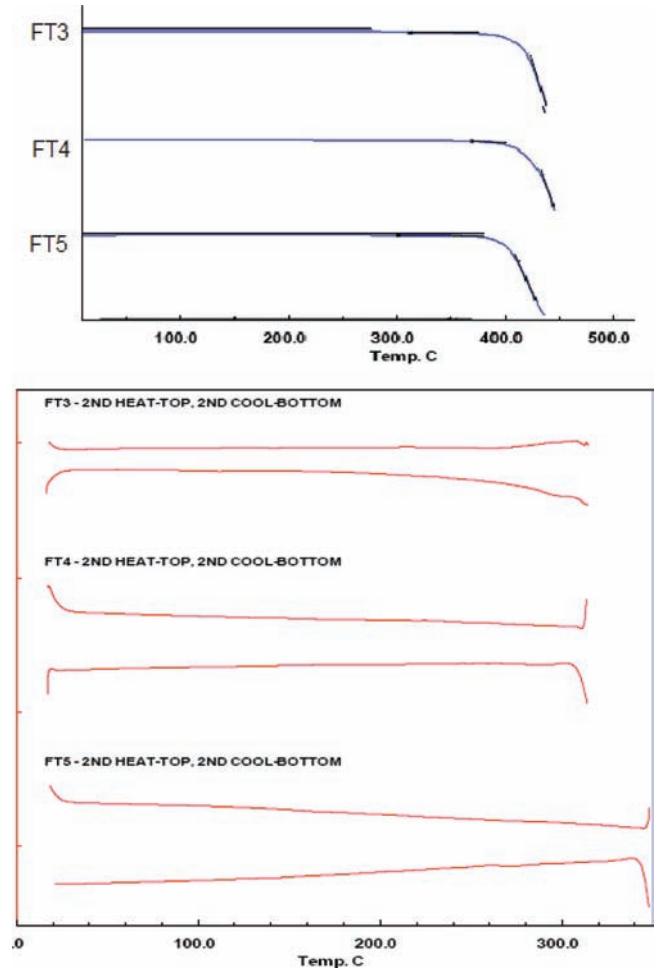

Figure 3. TGA and DSC[(a)] of FT3, FT4, and FT5 polymers.

cooling the sample to room temperature. The samples were then reheated at 5 °C/min using a Mettler hot stage starting at 75 °C. After the samples were reheated to around 150 °C, we found that the P2TDC10FT4 polymer became soft enough that the cover glass could be moved when pushed from the edge with a spatula. At temperatures below 130 °C, the coverslip would simply separate from the polymer if pushed too hard, not sheared. However, the polymers never became isotropic even when heated to the hot stage limit at 360 °C. During the heating period, birefringence was observed through this process.

We believe that the polymers retain a highly ordered packing on which we will elucidate more in the X-ray section. However, we could not find any transition peaks from DCS for the softening transition of the polymers, no matter if the ramp speed was 1 or 5 °C/min.

Grazing Incidence X-ray Scattering. For GIWAXS measurements, samples were prepared by spin-casting pentachloroethane solutions of polymers (3 mg/mL) at 1500 rpm on silicon wafers with a 300 nm oxide layer. Subsequently, the samples were annealed at 150 °C for 30 min. Acquired 2-D GIWAXS patterns are shown in Figure 4, while Figure 5 shows the extracted scattering intensities along the q_z and q_{xy} directions.

The GIWAXS images from the three samples are consistent with the formation of lamellae parallel to the substrate in all cases. The most striking difference in the X-ray scattering data between P2TDC10FT4 on one hand and P2TDC10FT3 and P2TDC10FT5 on the other is the drastic change in lamellar

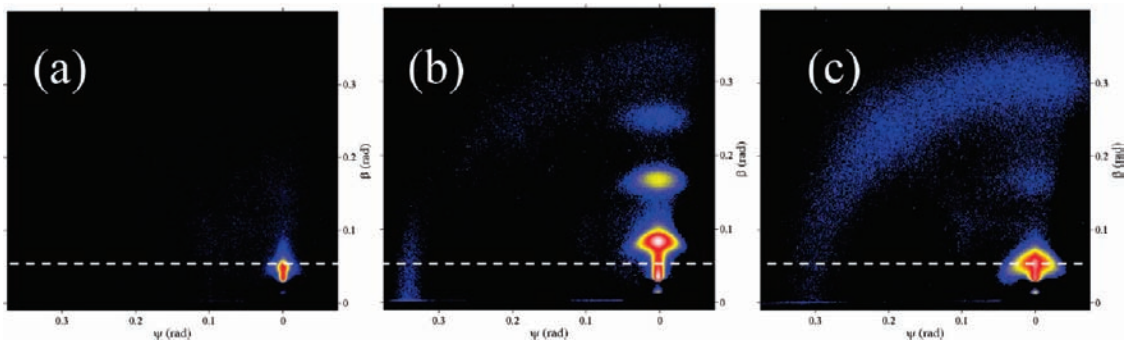

Figure 4. 2-D GIWAXS patterns of the thin films of (a) FT3, (b) FT4, and (c) FT5 cast on SiO_2 surface upon annealing. The dashed line marks the first order lamellar reflections of FT3 and FT5, and highlights the significant difference to the FT4 lamellar spacing.

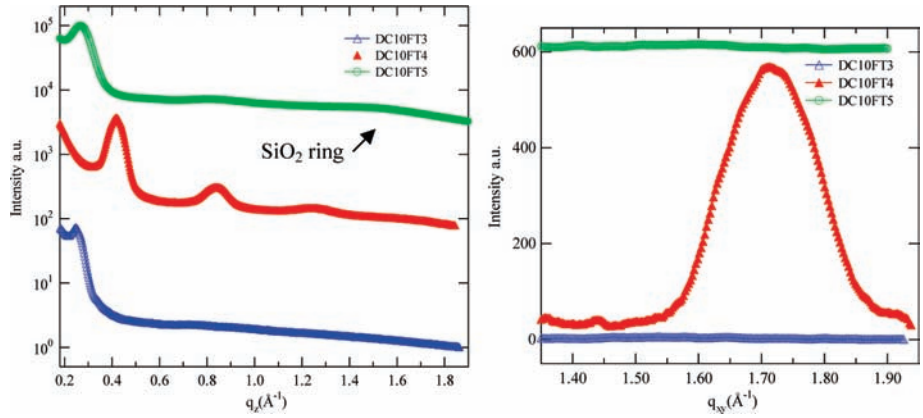

Figure 5. GIWAXS patterns of the polymer film cast on SiO_2 surface in (a) q_z and (b) q_{xy} direction for FT3, FT4, and FT5 upon annealing.

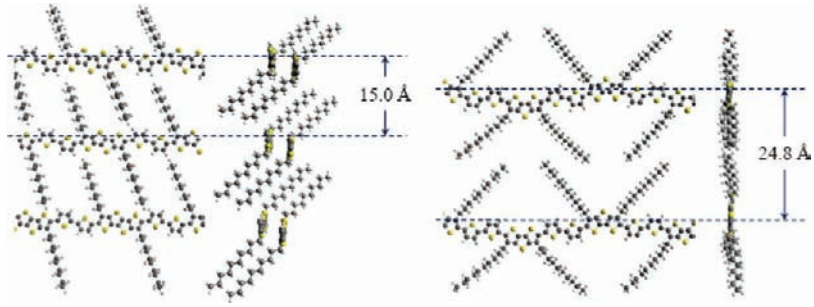

Figure 6. Proposed stacking for even-numbered tetrathieneoacene (left), as opposed to odd-numbered tetrathieneoacene (right).

spacing. Lamellae spacings were determined as 24.8, 15.0, and 22.8 Å for P2TDC10FT3, P2TDC10FT4, and P2TDC10FT5, respectively. The P2TDC10FT4 lamellar spacing is even smaller than in P3HT (16 Å), leaving very little space for the decyl side chains. This finding seems to indicate that the side chains point out-of-plane which is consistent with some other recent results. Baeuerle and co-workers analyzed the crystal structure of a 12-ring thiophene oligomer with dodecyl side chains.[27] They found that both the backbone and the side chains were rotated out of the main plane given by the monomer repeat and the lamellar distance, while the molecules as a whole remained relatively planar. A combined experimental and theoretical study[13,28,29] concluded for p3HT, PQT, and pBTTT that the backbone planes as well as the side chains are tilted out of the main plane. P2TDC10FT4 is very similar in its side chain arrangement, while P2TDC10FT3 and P2TDC10FT5 have two side chains on the same side of the fused ring which apparently demands a different packing.

In Figure 6, we show some possible side chain arrangements that can explain the observed lamellar spacing. For P2TDC10FT3 and P2TDC10FT5, there appears to be at best small out-of-plain tilt angles. The side chain arrangement was chosen to reflect the tendency of alkanes to form a dense packing. Note that any such packing must have a high degree of disorder considering the observed X-ray scattering from such films. In contrast, P2TDC10FT4 appears to behave much more like P3HT or PBTTT. However, in contrast to PBTTT, it does not show a phase transition in DSC.

As observed, there are no peaks along the q_{xy} direction for P2TDC10FT3 and P2TDC10FT5, indicating poor in-plane ordering. The in-plane peak for P2TDC10FT4 corresponds to

(27) Azumi, R.; Mena-Osteritz, E.; Boese, R.; Benet-Buchholz, J.; Baeuerle, P. *J. Mater. Chem.* **2006**, *16*, 728.
(28) DeLongchamp, D. M.; Kline, R. J.; Lin, E. K.; Fischer, D. A.; Richter, L. J.; Lucas, L. A.; Heeney, M.; McCulloch, I.; Northrup, J. E. *Adv. Mater.* **2007**, *19*, 833.
(29) Northrup, J. E. *Phys. Rev. B* **2007**, *76*, 245202.

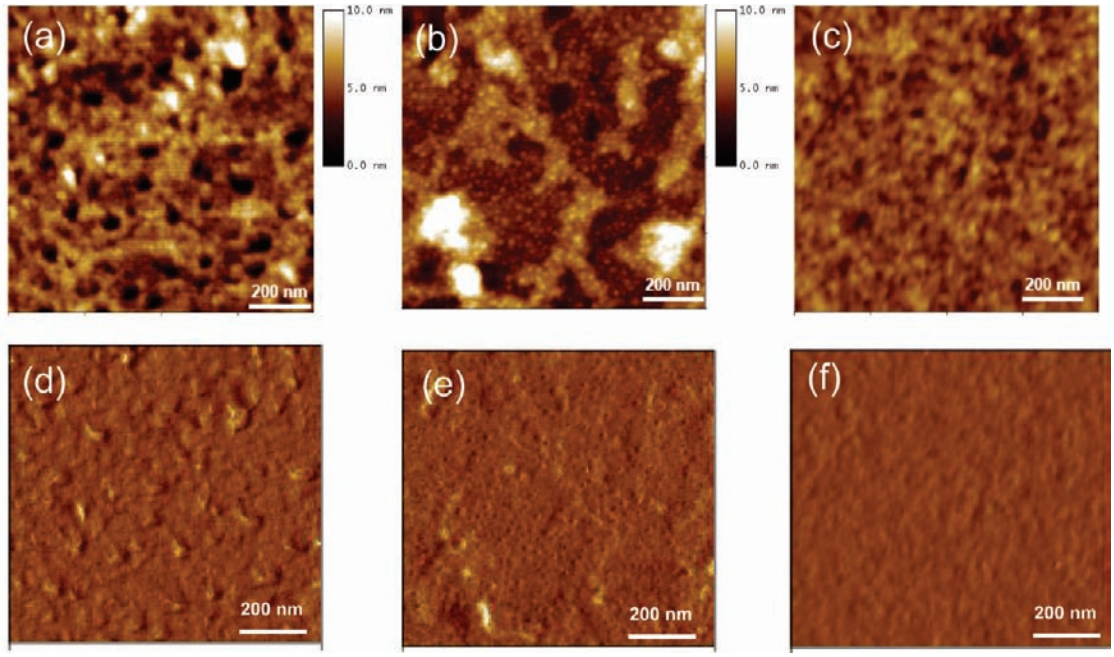

Figure 7. Tapping mode AFM images for a 1 × 1 μm^2 scan area of (a and d) P2TDC10FT3, (b and e) P2TDC10FT4, and (c and f) P2TDC10FT5 on the OFET devices after annealing at 150 °C for 30 min. The upper row (a−c) shows topographic images and the lower row (d−f) shows phase contrast images.

3.65 Å, which can be assigned to the $\pi-\pi$ stacking distance. This is a crucial parameter for electronic transport in the materials and is comparable to values observed for PQT (3.7 Å),[30] PBTTT (3.67−3.71 Å),[13] and PTzQT (3.5−3.7 Å).[16] It seems possible to improve the transport in fused polythiophenes by increasing the fused backbone length; however, as shown in this work, careful attention must be paid to design the right symmetrical molecular and regioregular structures, in order to achieve adequate crystalline packing.

Morphological Study of the Polymer Thin Films. The morphology of the polymer thin films on the transistor surface (annealed at 150 °C) was studied using tapping mode atomic force microscopy (AFM). Figure 7 shows AFM images of the polymer thin films inside the channel of transistors after annealing, where the upper row (Figure 7a−c) shows topographic images and the lower row (Figure 7d−f) shows phase contrast images. AFM images for all polymers show that uniform and flat films with rms roughnesses of ∼1−2 nm were obtained. P2TDC10FT4 films form large molecular terraces, where the molecular step height corresponds to the lamellar spacing measured by XRD. These terraces have domain sizes of ∼100−200 nm and are a direct visualization of the π-stacked lamella structure inferred from XRD results. The morphology of FT4 films that display large domains is very similar to that of PQT and PBTTT, which affords large crystalline domains with extended smooth, terracelike structures evidently rooted in their lamellar morphologies.[10,30]

P2TDC10FT3 films form domains of around 50 nm. The smaller domain size is likely a result of the fact that the P2TDC10FT3 polymer film has a smaller fused thiophene core and less side chain interactions compared to the P2TDC10FT4 film. On the other hand, P2TDC10FT5 has a moderately ordered structure with weak terracing as shown in Figure 7c. The domains are considerably smaller than the domains observed for P2TDC10FT4. However, the small domains in the P2TDC10FT5 morphology seem to be well-connected with each other, diluting the disordered regions, and are packed into isotropic amorphous-like superstructures. All of these morphologies for P2TDC10FT*n* (n = 3, 4, 5) films are in sharp contrast to those of rrP3HT, which affords a nanofibrillar morphology.[31−33]

The reduced ordering in the series FT4 > FT5 > FT3 is consistent with the other structural measurement and charge carrier mobility results. This trend is more obvious in the 5 × 5 μm^2 scan area AFM images in the Supporting Information.

OFET Properties. OFET properties of the polymers were evaluated using top contact devices fabricated by spin-casting the room temperature pentachloroethane solution of the polymers on the SiO_2 gate dielectrics, which were treated by octyltrichlorosilane (C8OTS) or hexamethyldisilazane (HMDS).

Figures 8−11 show the typical current−voltage characteristics of polymeric OFET devices with a channel length (L) = 80 μm, where I_{SD}, V_{SD}, and V_G represent source-drain current, source-drain voltage, and gate voltage, respectively. The saturation region field-effect mobility (μ) was calculated from the transfer characteristics of the OFETs using the slope derived from $(-I_{SD})^{1/2}$ versus V_G plots between −100 and −60 V (Figures 8−10). The threshold voltages (V_{TH}) of different polymer OFETs were derived from the onset of the transfer curves. The output curves (Figure 11) of polymers with different number of fused thiophene member cores show good saturation and linear behavior in the range of lower V_{SD}.

The linearity of the output curves in the low V_{SD} regime (0 to −5 V) indicates that Au forms an ohmic contact with polymers. Mobility values, on/off ratios, and threshold voltages

(30) Ong, B. S.; Wu, Y.; Liu, P.; Gardner, S. *J. Am. Chem. Soc.* **2004**, *126*, 3378.
(31) Zen, A.; Pflaum, J.; Hirschmann, S.; Zhuang, W.; Jaiser, F.; Asawapirom, U.; Rabe, J. P.; Scherf, U.; Neher, D. *Adv. Funct. Mater.* **2004**, *14*, 757.
(32) Kline, R. J.; McGehee, M. D.; Kadnikova, E. N.; Liu, J.; Fréchet, J. M. J. *Adv. Mater.* **2003**, *15*, 1519.
(33) Yang, H.; Shin, T. J.; Yang, L.; Cho, K.; Ryu, C. Y.; Bao, Z. *Adv. Funct. Mater.* **2005**, *15*, 671.

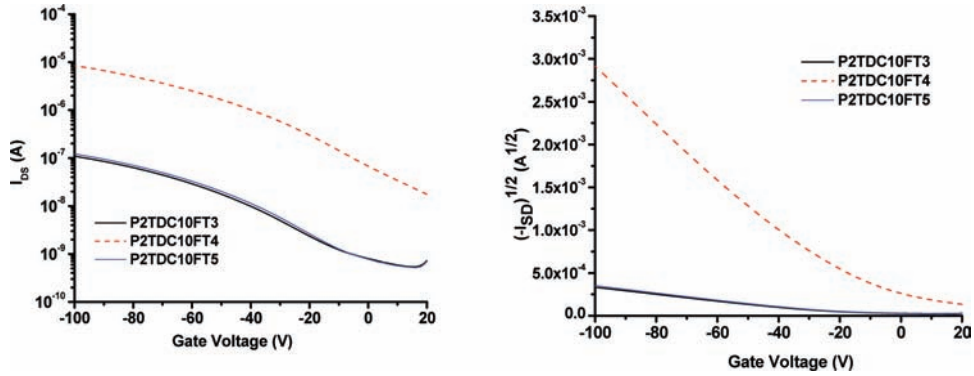

Figure 8. Transfer characteristics of the annealed polymer devices on bare SiO_2/Si for P2TDC10FT3, P2TDC10FT4, and P2TDC10FT5 at $V_{SD} = -80$ V.

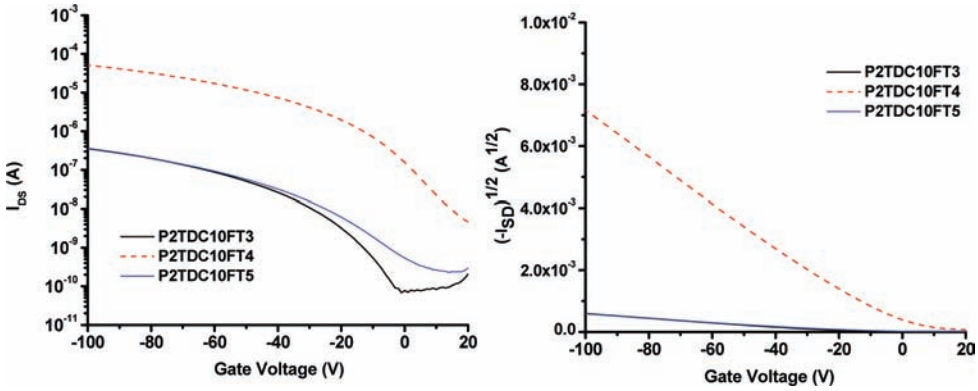

Figure 9. Transfer characteristics of the annealed polymer devices on C8OTS treated SiO_2/Si for P2TDC10FT3, P2TDC10FT4, and P2TDC10FT5 at $V_{SD} = -80$ V.

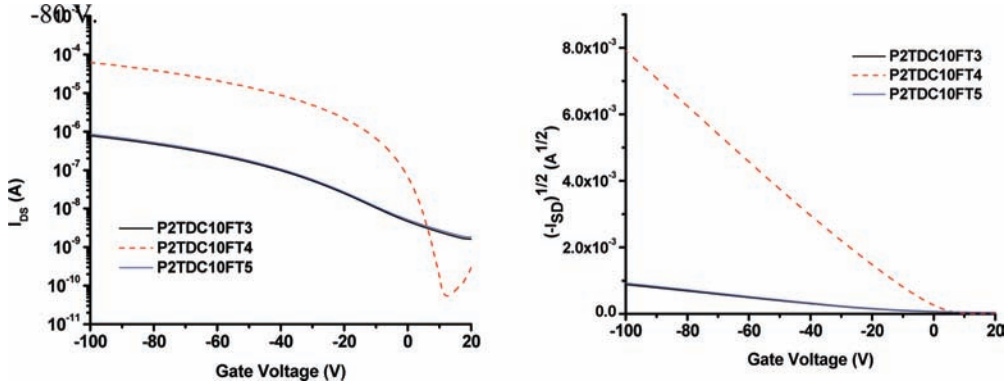

Figure 10. Transfer characteristics of the annealed polymer devices on HMDS treated SiO_2/Si for P2TDC10FT3, P2TDC10FT4, and P2TDC10FT5 at $V_{SD} = -80$ V.

of the polymer devices for P2TDC10FT*n* ($n = 3, 4, 5$) on different SiO_2 surfaces are summarized in Table 3. All polymer devices showed very good reproducibility and low deviation values, which indicates the excellent uniformity of the polymer thin films. OFET characteristics of polymers on differently treated surfaces are shown in the figures.

On the basis of our X-ray and polymer morphology studies, it is no surprise that polymers with a four members fused thiophene core showed the highest mobility among the polymers with the identical side alkyl chain. Mobility data of all three polymers are listed in Table 3.

From the table, the P2TDC10FT4 polymer gave the highest mobility values on all different treated silicon wafers. However, the 0.087 and 0.078 mobility values obtained from HMDS and C8OTS treated surfaces is about 4-fold smaller than our reported best value.[19] We believe that this may be due to the chain length effect, solvent effect, and P2TDC10FT4 polymer solubility limitation. On the other hand, three and five member fused thiophene core based polymers showed one or two order magnitude lower mobility values than the analogous four member fused thiophene, which is due to their poor lamellar packing orderings revealed in the GIWAXS study.

The devices on C8OTS and HMDS treated SiO_2/Si substrates exhibited one order magnitude higher mobility, two or 3 orders of magnitude higher on/off ratio, and much lower threshold voltage than the devices on bare substrates. For instance, OFET devices based on P2TDC10FT4 on HMDS-treated SiO_2 dielectrics showed a higher average μ value of 0.072 $cm^2/(V\ s)$, higher

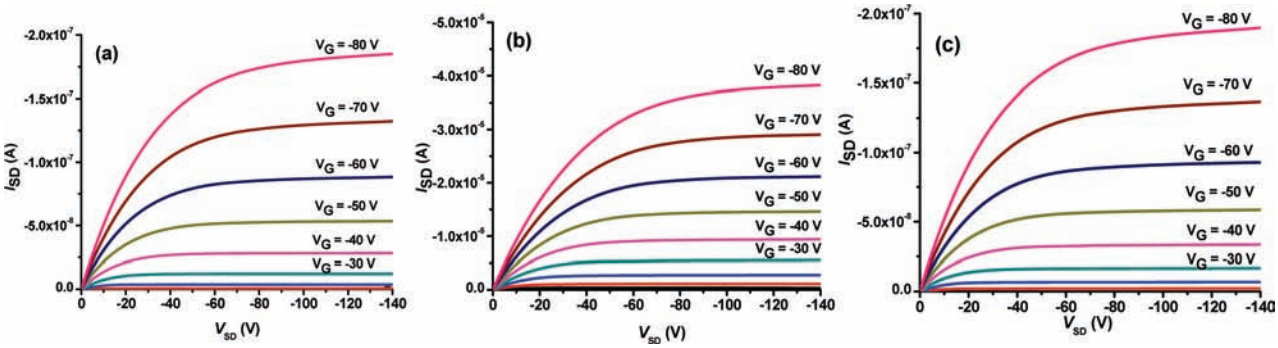

Figure 11. Output curves of the annealed polymer devices on C8OTS treated SiO_2/Si for (a) P2TDC10FT3, (b) P2TDC10FT4, and (c) P2TDC10FT5 at different gate voltages.

Table 3. Device Performance of P2TDC10FT3, P2TDC10FT4, and P2TDC10FT5 Polymers on Different Surfaces

polymer	surface treatment	maximum mobility (cm^2/(V s))	average mobility of 40 devices (cm^2/(V s))	deviation (cm^2/(V s))	on/off ratio	Vt (V)
P2TDC10FT3	Bare	0.00017	0.00011	0.000014	10^2	−13
	OTS	0.00063	0.00050	0.00011	10^3−10^4	−10
	HMDS	0.0017	0.001	0.00071	10^3	−11
P2TDC10FT4	Bare	0.015	0.010	0.00064	10^3	−10
	OTS	0.078	0.065	0.0058	10^4−10^5	−4
	HMDS	0.087	0.072	0.0051	10^6	−4
P2TDC10FT5	Bare	0.00019	0.00015	0.000018	10^2−10^3	−12
	OTS	0.00068	0.00055	0.00007	10^3−10^4	−11
	HMDS	0.0023	0.0015	0.00053	10^3−10^4	−9

$I_{on}/I_{off} > 10^6$, and lower $V_{th} \approx -4$ V, compared with the devices on bare substrates having an average μ value of 0.01 cm^2/(V s), $I_{on}/I_{off} \approx 10^3$, and $V_{th} \approx -10$ V. This indicates that alkylsilane self-assembled monolayers on oxide surfaces can be used to decrease the oxygen doping into the polymer film, decrease the trap sites, and improve the molecular chain packing order of the polymer semiconductor at the gate dielectric/semiconductor interface for the fused thiophene polymers.

4. Conclusion

To systematically study the structure−property relationships in polythienothiophenes with different fused ring size and the side chain impact on polymer backbone packing, we have successfully synthesized P2TDC10FT3, P2TDC10FT4, and P2TDC10FT5 polymers. Optical spectra suggest that all of these polymers have their conjugated units well-extended through their polymer backbone, no matter whether the fused ring size is smaller or larger. Cyclic voltammetry showed that all three polymers have large IP values, which indicates they are oxidatively more stable than rrP3HT and PBTTT. Thermal analysis proved that these polymers can tolerate temperatures of up to 400 °C before decomposing. These properties provides a big processing window for real commercial applications.

DSC analysis indicates all three polymers have no liquid crystalline phase transitions. A GIWAXS study confirmed that P2TDC10FT4 can form tighter lamellae packing structures due to proper side chain arrangements. On the other hand, P2TDC10FT3 and P2TDC10FT5 polymer backbones packed much more loosely because of their side chain interference. AFM images were consistent with the X-ray scattering results. The P2TDC10FT4 polymer demonstrated the largest terrace structure among all three polymers. It is no surprise that the P2TDC10FT4 polymer gives the best device performance. By properly coating a wafer surface with an organic monolayer, polymer packing can be further enhanced which resulted in higher mobility values.

Through this systematic study, we also can draw the following important conclusions: (1) alkylsubstituted even-numbered fused thiophene ring polymers can form proper packing structures which have better performance than odd-numbered fused thiophene ring polymers; (2) a regioregular structure with side chains pointing in opposite directions is preferable to yield high mobilities; (3) larger conjugation units are better able to form self-assembled structures, when even-numbered or odd-numbered fused ring structures are compared separately. In our case, P2TDC10FT4 can form aggregates without a careful annealing process which is crucial for large-scale production. When comparing P2TDC10FT3 with P2TDC10FT5, the latter has a larger conjugation unit, which results in improved backbone packing and somewhat smaller interlamellar distances.

Acknowledgment. The authors would like to thank Dr. Thomas, M. Leslie for polarized microscopy experiments. We thank the reviewers for carefully examining our work and making valuable suggestions. Financial support was provided by Corning Incorporated. Part of the work was performed at the Cornell NanoScale Facility and the Cornell High Energy Synchrotron Source. CHESS is a national user facility which is supported by the National Science Foundation and the National Institutes of Health/National Institute of General Medical Sciences under NSF award DMR-0225180.

Supporting Information Available: Additional AFM images, GPC results, ^{1}H NMR results and the complete author list of ref 11. This material is available free of charge via the Internet at http://pubs.acs.org.

JA903895S